UC-25

To be Submitted for Publication

LBL-7354
Preprint

EROSION IN A CURVED PIPE

Woon-Shing Yeung

September 1977

Prepared for the U. S. Department of Energy
under Contract W-7405-ENG-48

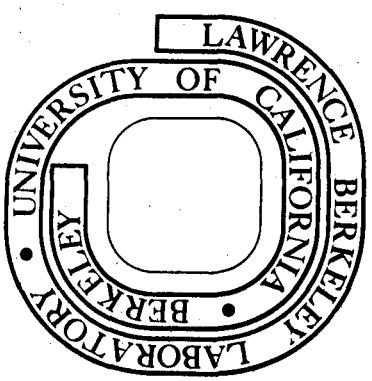

DISCLAIMER

LBL-7354

EROSION IN A CURVED PIPE

Woon-Shing Yeung

Materials and Molecular Research Division
Lawrence Berkeley Laboratory
University of California
Berkeley, California 94720

ABSTRACT

The erosion in a curved pipe carrying a gas-particle mixture has been investigated. The fluid mechanics of such a system were solved under several idealized assumptions to obtain information about impact velocities, impingement angle, and mass of particles striking per unit time per unit area. The results have been presented in terms of the maximum relative erosion rate at the central plane of the curved pipe, and it has been found that, under the assumptions used, the maximum relative erosion rate E_{max} can be expressed as proportionate to $W^3 Z_L$ for large W and to $W^{3.93} Z_L$ for small W, where W is the initial flow velocity of mixture and Z_L is the loading ratio (in mass of particles/mass of gas).

LIST OF SYMBOLS

Capital Letters:

A	area element
D	distance traveled in cell
D/d	curvature ratio used in Reference 8
E	relative erosion per unit time per unit area
E_{max}	maximum relative erosion rate per unit area at the central plane of the curved pipe
F( )	functional designation
$\underset{\sim}{F}$	column vector
Fr	Froude number
$\tilde{L}_m$	non-dimensional momentum equilibration length, $W\tau_m/a$
M	local mass of particles striking per unit time per unit area
N	number flow rate of particles in particles/sec
P	number of particles in cell
Q	impact velocity
$\underset{\sim}{Q}$	impact velocity vector
R	mean radius of pipe axis
Re	Reynolds number
S	equation for pipe surface
U	initial velocity
V	characteristic velocity
V_{rel}	relative speed of particle to fluid
VCELL	volume of cell
W	entry velocity of curved pipe flow
$\underset{\sim}{Y}$	column vector

Z	particle loading in % by weight of particles in mixture
Z_L	particle loading in mass particle/mass gas

Small letters:

a	pipe radius
d_p	particle diameter
$(\underset{\sim}{e}_r, \underset{\sim}{e}_\psi, \underset{\sim}{e}_\phi)$	unit vector for toroidal coordinates
f	number of particles per unit volume of mixture
g	acceleration due to gravity
n	exponent for Q in erosion correlation
$\underset{\sim}{n}$	outward normal vector for pipe surface
(n,m)	grid designation at initial plane
(r,ψ,ϕ)	coordinate variables for toroidal system
$(\bar{r},\bar{\psi},\bar{\phi})$	non-dimensional coordinates for toroidal system
t	time coordinate
$\bar{t}$	non-dimensional time coordinate
(u,v,w)	velocity components
$(\bar{u},\bar{v},\bar{w})$	non-dimensional velocity components
w	mean wear rate, used in Ref. 8

Greek letters:

α	impingement angle
δ	curvature ratio
λ	average interparticle distance
ρ	material density
$\bar{\rho}$	phase density at wall
σ	particle radius

ν	kinematic viscosity
μ	viscosity
τ	residence time in cell of particle stream
τ_m	momentum equilibration time
$\underset{\sim}{\nabla}$	gradient operator
Δ	small quantity
Γ	particle volume

Subscripts:

f	fluid variables
i	value relating to impact
k	index for particle trajectory
max	maximum value
0	initial conditions
p	particle variables

INTRODUCTION

Erosion has been observed in various vessels and components that handle gas-particle flow. Many components fail at an earlier stage than expected because erosion is not adequately accounted for in the design process.

The mechanisms and factors governing the rate of erosion have attracted wide interest during the last decade. Finnie[1] has derived a formula relating the volume removal of the eroded surface to several parameters of the eroding particles, among which are the impact velocity, impingement angle and mass of particles striking the surface per unit time and unit area. It is therefore necessary to solve for the particle trajectories and particle density at the surface being eroded in order to determine accurately the rate of erosion. This calls for investigation of the fluid dynamics of the gas-particle two phase flow in certain geometries, particularly flows through a pipe bend, which is a common component in many piping systems.

THEORY

The problem of general gas-particle flow is notoriously complicated and there are only a few analytical solutions, most of which are for flow over a semi-infinite flat plate. For a rather complete bibliography, see Soo.[2] The problem becomes more difficult when one considers the gas-particle flow through a curved pipe. Here the flow field becomes complex because of the secondary flow resulting from the three dimensional pipe bend.

In order to simplify the problem as much as possible, the following assumptions have been made:

(a) The particle loading is sufficiently small so that particle-particle interaction is negligible compared with particle-fluid interaction. This is true when the average interparticle distance is large compared with the size of the particle. If we assume each particle is spherical with a diameter d_p, and denote the material density of the particles by ρ_p, the material density of the fluid by ρ_f, and the particle loading in mass of particles per unit mass of fluid by Z_L, we can approximate the average interparticle distance by

$$\lambda = d_p \sqrt[3]{\frac{\rho_p}{Z_L \rho_f}}$$

The material density ratio of the particle and the fluid is about 1000 for many practical cases, so that the interparticle distance can be roughly 10 times the particle diameter for a loading ratio of about 1. Furthermore, since the mixture is assumed dilute, the volume fraction of the particle phase is much less than unity, and we can neglect the volume occupied by the particles.

(b) The presence of the particles does not influence the gas flow field. This is the so-called "one-sided momentum coupling" assumption and is justified because the mixture is very dilute.

(c) Of all the forces that act on the particle, only the aerodynamic drag force caused by a difference in velocity of the fluid and particle phase is significant. The gravity force can be neglected since the particle Froude number, defined as

$$Fr_p = \frac{V_p^2}{2g\sigma}$$

where V_p is a characteristic velocity of the particle and σ is the particle radius, is usually very large under normal circumstances. Other negligible forces include the pressure force in the gas flow field, the virtual mass effect, and the shear stress of a particulate cloud, etc. This assumption greatly simplifies the equation of motion of the particle, which is rather complicated in its general form.[3]

(d) The drag force is assumed to be given by Stokes law throughout the analysis. This holds true when the particle Reynolds number, based on the relative speed V_{rel} of the particle to the fluid, is less than or of order unity. Hence, we assume

$$Re_p = \frac{V_{rel}\,\sigma}{\nu_f} \lesssim O(1)$$

where ν_f is the kinematic viscosity of the fluid.

(e) The gas-particle mixture enters the curved pipe with a uniform velocity. The particles are assumed to be in dynamic equilibrium with the gas and are distributed uniformly through the gas on entering the pipe with a loading ratio Z in percent by weight of particles in the mixture. Furthermore, if the Dean number* of the flow is large, the uniform region is negligibly perturbed except for a thin boundary layer near the wall;[4] we can assume the motion of the gas is uniform throughout the bent section of the pipe (i.e. a slug flow model).

Having listed the assumptions used in the analysis, we shall proceed to formulate the fluid dynamics of the two phase flow system. We choose a set of toroidal coordinates (r,ψ,ϕ) as shown in Fig. 1. Denote the

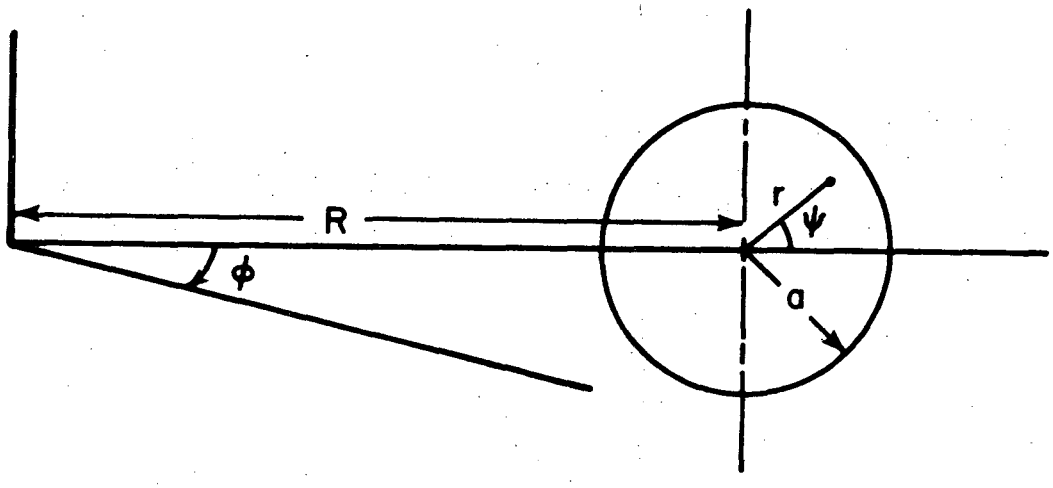

Figure 1. Toroidal coordinate system.

* Dean number is defined here as $Re(a/R)^{1/2}$. See Fig. 1

velocity by u in increasing r-direction, v in increasing ψ-direction and w in increasing ϕ-direction. In addition, we shall use the subscript f to denote values pertaining to the fluid phase and p to the particle phase. By virtue of assumption (e), we can write down the motion of the fluid corresponding to a slug flow model as

$$\begin{aligned} u_f &= v_f = 0 \\ w_f &= W \end{aligned} \tag{1}$$

where W is the initial velocity at $\phi = 0$.

We are now in a position to formulate the particle phase. This can be done using two approaches: (1) the Eulerian approach, in which the particles are treated as a continuum and conservation laws are formulated accordingly,[5] and (2) the Lagrangian approach in which attention is fixed upon a particular particle along its whole trajectory in the domain of interest. These two approaches lead to two rather different problems, both mathematically and conceptually. In most cases, the Eulerian approach is more difficult than the Lagrangian approach. In the case of a curved pipe, the Lagrangian technique is found to be easier than the Eulerian counterpart, at least from entry into the curve up to the first particle impact. (The phenomenon of multiple reflection within a curved pipe is problematic in both approaches.) We shall thus use the Lagrangian approach in our analysis here and leave the Eulerian formulation to a

separate report of the author. In view of assumption (c), the equations of motion for a single particle in toroidal coordinates are

$$\frac{du_p}{dt} - \frac{w_p^2 \cos\psi}{R+r\cos\psi} - \frac{v_p^2}{r} = -\frac{u_p}{\tau_m} \tag{2}$$

$$\frac{dv_p}{dt} + \frac{w_p^2 \sin\psi}{R+r\cos\psi} + \frac{u_p v_p}{r} = -\frac{v_p}{\tau_m} \tag{3}$$

and

$$\frac{dw_p}{dt} + \frac{u_p w_p \cos\psi}{R+r\cos\psi} - \frac{v_p w_p \sin\psi}{R+r\cos\psi} = \frac{W-w_p}{\tau_m} \tag{4}$$

taking into account the Coriolis and centripetal acceleration terms and making use of Eq. (1). In Eqs. (2) to (4), τ_m is known as the momentum equilibration time and can easily be shown to be equal to

$$\left(\frac{2}{9}\frac{\sigma^2 \rho_p}{\mu_f}\right) ;$$

and R is the mean radius of the pipe axis, as in Fig. 1. Furthermore, for a particle positioned at (r,ψ,ϕ), the Lagrangian velocity components are given by

$$\frac{dr}{dt} = u_p \tag{5}$$

$$\frac{d\psi}{dt} = \frac{v_p}{r} \tag{6}$$

$$\frac{d\phi}{dt} = \frac{w_p}{R+r\cos\psi} \tag{7}$$

The initial conditions are, at $\phi = 0$,

$$u_p = v_p = \phi = 0$$

$$w_p = W,\ r = r_0,\ \psi = \psi_0 \tag{8}$$

where $(r_0,\psi_0,0)$ is the initial position occupied by the particle whose trajectory we wish to compute. It is convenient for numerical analysis purposes to rewrite Eqs. (2) to (7) in matrix form. Thus, introduce column vectors Y and F, where

$$Y \equiv \begin{Bmatrix} u_p \\ v_p \\ w_p \\ r \\ \psi \\ \phi \end{Bmatrix} \tag{9}$$

$$F \equiv \begin{Bmatrix} \dfrac{w_p^2 \cos\psi}{R+r\cos\psi} + \dfrac{v_p^2}{r} - \dfrac{u_p}{\tau_m} \\ -\dfrac{w_p^2 \sin\psi}{R+r\cos\psi} - \dfrac{u_p v_p}{r} - \dfrac{v_p}{\tau_m} \\ \dfrac{W}{\tau_m} - w_p\left(\dfrac{u_p \cos\psi}{R+r\cos\psi} - \dfrac{v_p \sin\psi}{R+r\cos\psi} + \dfrac{1}{\tau_m}\right) \\ u_p \\ \dfrac{v_p}{r} \\ \dfrac{w_p}{R+r\cos\psi} \end{Bmatrix} \tag{10}$$

Equations (2) to (7) can be rewritten as, in matrix form,

$$\frac{d\underset{\sim}{Y}}{dt} = \underset{\sim}{F}(t;\underset{\sim}{Y}) \tag{11}$$

subject to the initial conditions

$$\underset{\sim}{Y} = \underset{\sim}{Y}_0 \tag{12}$$

where Y_0 is given in the present case by

$$\underset{\sim}{Y}_0 = \begin{Bmatrix} 0 \\ 0 \\ W \\ r_o \\ \Psi_o \\ 0 \end{Bmatrix}$$

Equation (11) together with initial condition (12) must then be solved numerically. In order to gain some quantitative insight into the problem before obtaining a numerical solution, it is always desirable to non-dimensionalize the governing equations. Therefore, we define the dimensionless variables as follows

$$
\begin{aligned}
\bar{u}_p &= \frac{u_p}{W} \\
\bar{v}_p &= \frac{v_p}{W} \\
\bar{w}_p &= \frac{w_p}{W} \\
\bar{t} &= \frac{t}{\tau_m} \\
\bar{r} &= \frac{r}{a} \\
\bar{\psi} &= \psi \\
\bar{\phi} &= \phi
\end{aligned} \tag{13}
$$

where a is the radius of the pipe.

Making use of (13), Eqs. (2) to (7) then become

$$
\frac{d\bar{u}_p}{d\bar{t}} - \tilde{L}_m \left[\frac{\bar{w}_p^{\,2}\cos\bar{\psi}}{\delta+\bar{r}\cos\psi} + \frac{\bar{v}_p}{\bar{r}} \right] = -\bar{u}_p \tag{14}
$$

$$
\frac{d\bar{v}_p}{d\bar{t}} + \tilde{L}_m \left[\frac{\bar{w}_p^{\,2}\sin\bar{\psi}}{\delta+\bar{r}\cos\psi} + \frac{\bar{u}_p\bar{v}_p}{\bar{r}} \right] = -\bar{v}_p \tag{15}
$$

$$
\frac{d\bar{w}_p}{d\bar{t}} + \tilde{L}_m\bar{w}_p \left[\frac{\bar{u}_p\cos\bar{\psi}-\bar{v}_p\sin\bar{\psi}}{\delta+\bar{r}\cos\bar{\psi}} \right] = 1 - \bar{w}_p \tag{16}
$$

$$\frac{d\bar{r}}{d\bar{t}} = \tilde{L}_m \bar{u}_p \tag{17}$$

$$\frac{d\bar{\psi}}{d\bar{t}} = \frac{\tilde{L}_m \bar{v}_p}{\bar{r}} \tag{18}$$

$$\frac{d\bar{\phi}}{d\bar{t}} = \frac{\tilde{L}_m \bar{v}_p}{\delta + \bar{r}\cos\bar{\psi}} \tag{19}$$

where $\tilde{L}_m$ and δ are given by

$$\tilde{L}_m = \frac{W\tau_m}{a} \tag{20}$$

$$\delta = \frac{R}{a} \tag{21}$$

It is thus shown that the particle trajectory is a function of two dimensionless parameters, $\tilde{L}_m$ and δ. Physically, $\tilde{L}_m$ is the dimensionless momentum equilibration length[2] and δ is the curvature ratio which distinguishes curved pipe flow from the corresponding straight pipe flow.

We can expand $\tilde{L}_m$ in the simple case when τ_m is given by Stokes drag law as

$$\tilde{L}_m = \frac{2}{9}\left(\frac{W\sigma}{\nu_f}\right)\left(\frac{\rho_p}{\rho_f}\right)\left(\frac{\sigma}{a}\right) \tag{22}$$

Equation (22) clearly indicates various effects that influence the trajectory. Since $\tilde{L}_m$ is a measure of how far a particle will travel before it is adjusted to the gas flow field, the larger the value of $\tilde{L}_m$, the larger the deviation of the particle trajectories from the gas streamlines. Fast moving (particle Reynolds number $\frac{W\sigma}{\nu_f}$ will be large), dense ($\frac{\rho_p}{\rho_f}$ will be large), and large particles (σ/a will be large) will be expected to be influenced less dramatically by the gas flow field, and their trajectories will deviate drastically from the gas streamlines.

EROSION CALCULATION

Finnie[1] has given a formula for calculating the relative erosion rate per unit area of surface being eroded as

$$E = M\, Q^n\, F(\alpha)$$

$$F(\alpha) = \sin(2\alpha) - 4\sin^2\alpha \qquad \alpha \leqslant 14°$$

$$F(\alpha) = \cos^2\alpha/4 \qquad \alpha > 14° \tag{23}$$

where M is the mass of particles striking per unit area and unit time;

Q is the magnitude of the impact velocity;

α is the impingement angle measured from the tangent plane of the impact location on the pipe wall;

E is the relative erosion per unit time and unit area; and

n is the exponent of the impact velocity and depends on the type of particles and material of surface being eroded.

For a curved pipe, the pipe surface is represented by the equation

$$S = r-a = 0 \tag{24}$$

Hence the normal to the pipe surface is given by the gradient of S, or

$$\underset{\sim}{n} = \underset{\sim}{\nabla} S = \underset{\sim}{e}_r \tag{25}$$

where $\underset{\sim}{\nabla}$ is given by, in toroidal coordinates[3],

$$\underset{\sim}{\nabla} \equiv \frac{\partial}{\partial r}\underset{\sim}{e}_r + \frac{1}{r}\frac{\partial}{\partial \psi}\underset{\sim}{e}_\psi + \frac{1}{R+r\cos\psi}\frac{\partial}{\partial \phi}\underset{\sim}{e}_\phi \tag{26}$$

with $\underset{\sim}{e}_r$, $\underset{\sim}{e}_\psi$, $\underset{\sim}{e}_\phi$ being the unit vector in r,ψ,ϕ directions respectively. If the impact velocity vector is denoted by $\underset{\sim}{Q}$, with components represented by u_i, v_i and w_i, then the angle between $\underset{\sim}{Q}$ and the normal vector $\underset{\sim}{n}$ is just

$$\underset{\sim}{Q}\cdot\underset{\sim}{n} = |\underset{\sim}{Q}|\ |\underset{\sim}{n}|\ \cos(\underset{\sim}{Q},\underset{\sim}{n})$$

or

$$\cos(\underset{\sim}{Q},\underset{\sim}{n}) = u_i/Q \tag{27}$$

In (27), $\cos(\underset{\sim}{Q},\underset{\sim}{n})$ represents the angle between the impact velocity $\underset{\sim}{Q}$ and outward normal $\underset{\sim}{n}$. The impingement angle is simply the complimentary angle of $\cos(\underset{\sim}{Q},\underset{\sim}{n})$, or

$$\alpha = \sin^{-1}(u_i/Q) \tag{28}$$

Since Q and α can be easily obtained from the solution of Eq. (11) subject to the initial conditions (12) for the calculation of E, it only remains to determine M. If we know the phase density of particles at the wall, then M is simply given by

$$M = \bar{\rho}_p Q \tag{29}$$

where $\bar{\rho}_p$ is the phase density of the particles. The determination of $\bar{\rho}_p$ from the solution of Lagrangian equations of motion is not trivial and will be discussed in the next section.

Numerical Solution

Having decided the kind of particle and gas one wants to work with, the flow conditions and the geometry of the pipe, one can evaluate τ_m and other parameters necessary for the numerical solution of (11). The initial particle distribution is discretized at a finite number of stations with a corresponding particle flow rate depending on its representative surface area, as shown in Fig. 2 by the shaded area. The number flow rate of particles is found for each station and is assumed constant along the trajectory, as is done in Crowe.[6]

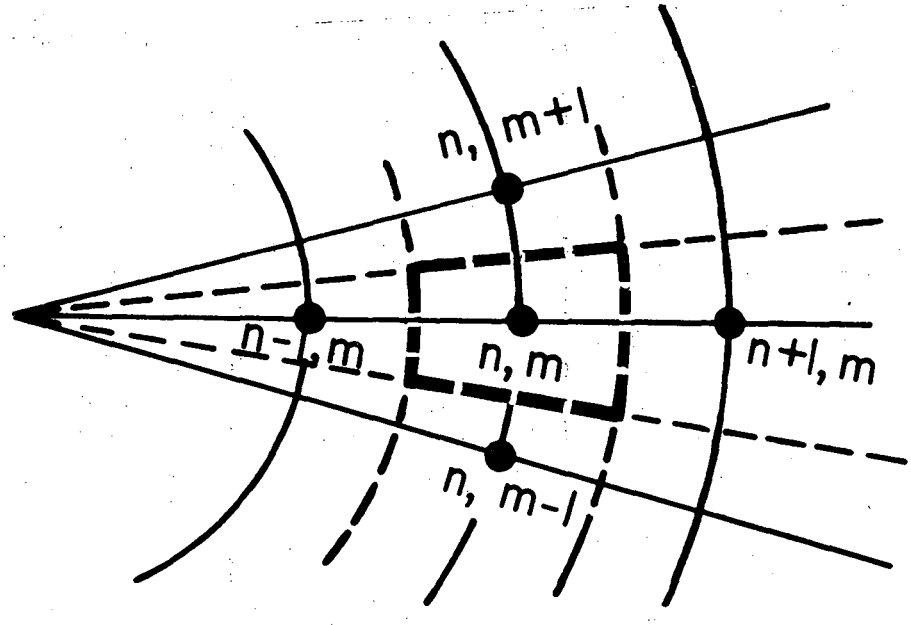

Figure 2. Grid representation.

Since the initial distribution of particles is uniform, and is characterized by Z% by weight of the particle in the mixture, the initial number density of a particle at $\phi = 0$ is then given by

$$f = \frac{Z}{\rho_p \Gamma} \frac{\rho_f}{1-Z} \tag{30}$$

where Γ is the volume of a particle

$$\Gamma = \frac{4}{3}\pi\sigma^3 \tag{31}$$

Thus the number flow rate at station (n,m) is given by

$$N = f\, W\, A(n,m) \tag{32}$$

with A(n,m) denoting the surface area with center at station (n,m). N will be different for different stations because A(n,m) changes over the initial plane $\phi = 0$ in general. Having determined N and solutions for particle trajectories, for all n and m, we can approximate the wall particle phase density $\overline{\rho}_p$ using a technique employed by Crowe.[6] We begin by dividing the immediate neighborhood of the pipe wall into cells of volume represented by VCELL; one of such cells is shown in Fig. 3.

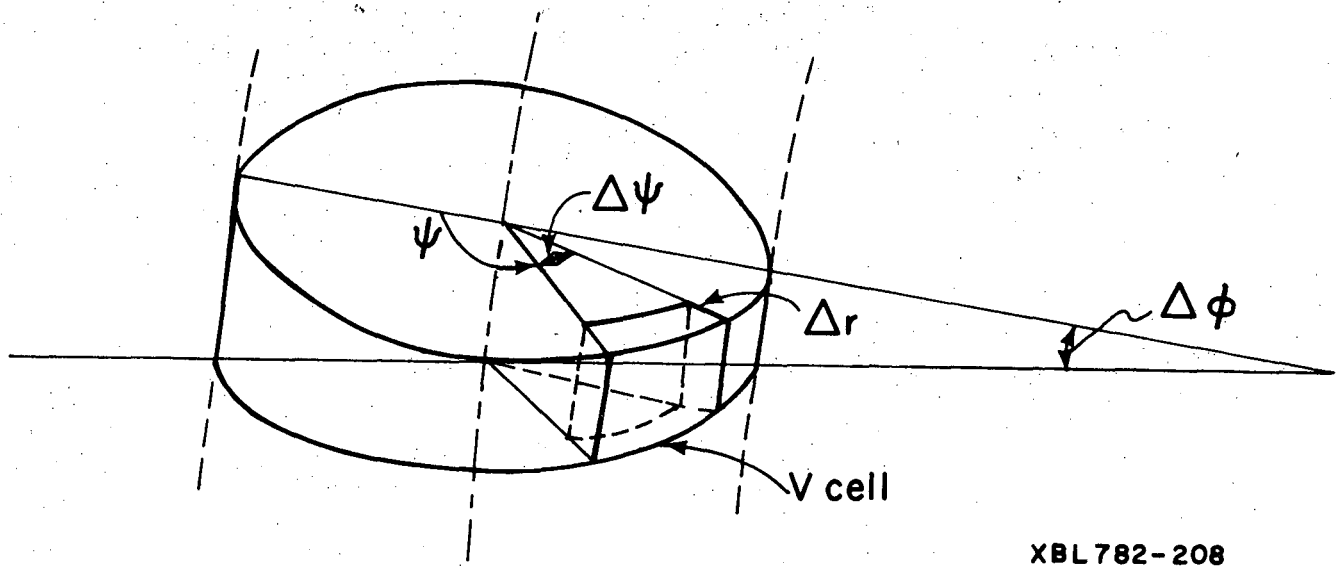

Figure 3. Cell designation at wall.

Thus VCELL is given by, for Δr, $\Delta\psi$, $\Delta\phi$ small,

$$VCELL = (R+a\cos\psi)\ (a)\ (\Delta r)\ (\Delta\psi)\ (\Delta\phi) \tag{33}$$

From the particle trajectories solution, we can compute the total number of particles in a particular cell by knowing the residence time in the cell of each particle trajectory that intersects the cell, and sum up all such trajectories. Thus if there are a total of i particle trajectories that intersect a particular cell, the total number of particles in that cell is

$$P = \sum_{k=1}^{i} N_k \tau_k \tag{34}$$

where N_k is the number flow rate of the kth particle trajectory. This is given by (32) because we can trace back the point from which this kth particle trajectory originates and τ_k is the corresponding residence time of the kth particle path. The mean particle phase density over the cell volume is then

$$\bar{\rho}_p = \frac{P\, m_p}{VCELL} \tag{35}$$

where m_p is the mass of a particle. Since VCELL is necessarily finite for numerical purposes, (35) does not give the actual local particle phase density, which is defined at a point, or as VCELL approaches zero. However, it is erroneous to assume that the smaller the VCELL we choose, the closer the mean particle phase density will approximate the local particle phase density, since we do not have a continuous distribution of particles at the first place. (Recall the discretization process at ϕ =0).

To illustrate this, suppose a uniformly distributed particle-gas mixture enters the initial plane with a uniform velocity U. (Fig. 4) We further assume that the particle paths are all perpendicular to the initial plane and the boundary. The initial particle distribution is then discretized to, say, 4 stations, each having a particle flow rate of N particles/sec. The thickness of the cells is Δy and we consider unit depth in the direction perpendicular to the plane of the paper so that the size of each cell is dependent on the size of ℓ we choose. For this simple case, the residence time is the same for all particle paths, and will be denoted by τ. The following graph shows the effect of the choice of ℓ (hence the choice of VCELL) on $\bar{\rho}_p$ at the boundary. (Fig. 5)

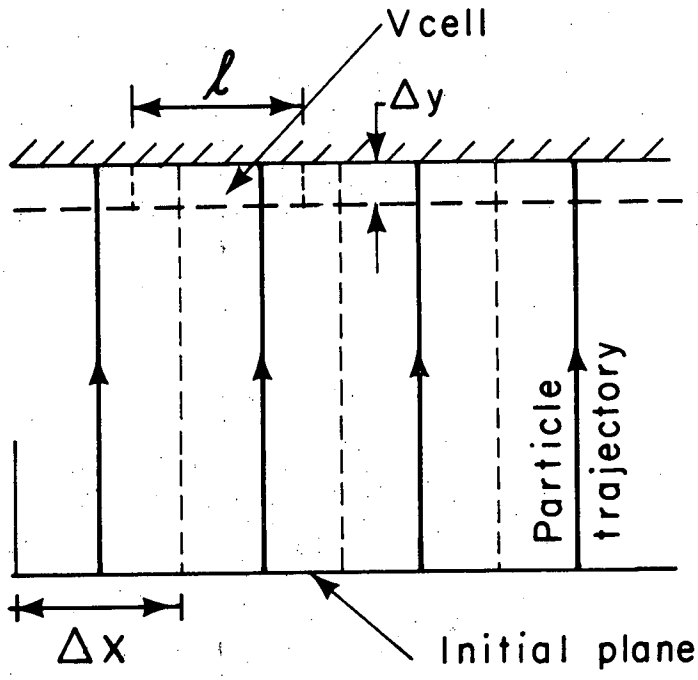

XBL782-207

Figure 4. Flow system of example.

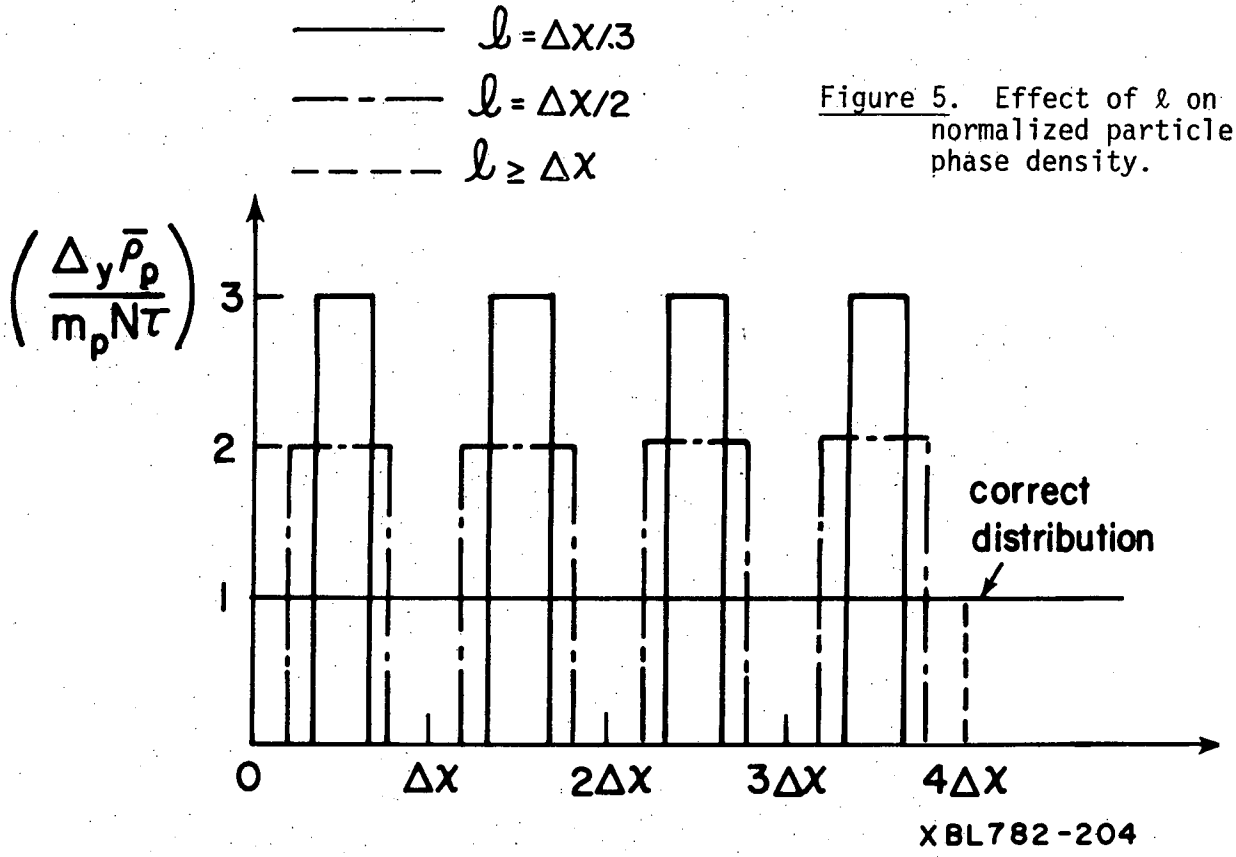

XBL782-204

Figure 5. Effect of ℓ on normalized particle phase density.

We know from the conditions given that the particle phase density should be uniform everywhere, particularly at the boundary. Figure 5 shows that for $\ell < \Delta x$, the normalized particle density distribution $\frac{\Delta y \bar{\rho}_p}{m_p N \tau}$ becomes more and more irregular, and for $\ell \geq \Delta x$, we obtain the correct particle distribution at the wall. This simple example at least suggests that the grid size at the boundary surface should be compatible with the initial grid size and in no case smaller than the initial grid size. Thus the accuracy of computing $\bar{\rho}_p$ at the boundary surface is actually restricted by the initial discretization scheme and approaches the real point particle phase density when one considers every individual particle entering the initial plane.

In the case of the curved pipe where the geometry is much more complicated than the example given above, the criterion for choosing the grid size at the pipe surface is the same as mentioned above. However, it is found useful to use a much larger grid size at the boundary than that at the initial plane so as to obtain a smooth distribution.

Let us return to the determination of M, the mass of particles striking per unit time and unit area at a certain location. Consider the kth particle trajectory intersecting the cell corresponding to that location. From Eq. (29), the value of M due to this kth stream is

$$M_k = \left(\bar{\rho}_p\right)_k Q_k = \left(\frac{m_p}{VCELL}\right) P_k Q_k \qquad (36)$$

where the subscript k refers to the kth particle stream and P_k is the number of particles in the cell due to the kth particle trajectory, as in (34). The total mass of particles striking per unit time and unit area is then approximately given by

$$M = \frac{m_p}{VCELL} \sum_{k=1}^{i} P_k Q_k \tag{37}$$

assuming there are i particle streams intersecting the cell. Similarly, one can compute the relative erosion rate due to each particle stream that enters the particular cell by means of Eq. (23). Making use of (37) we obtain

$$E_k = \left(\frac{m_p}{VCELL}\right) P_k Q_k^{n+1} F(\alpha_k) \tag{38}$$

The total relative erosion rate is then approximately

$$E = \frac{m_p}{VCELL} \sum_{k=1}^{i} P_k Q_k^{n+1} F(\alpha_k) \tag{39}$$

It is important to use the correct form of $F(\alpha_k)$ according to Eq. (23). We shall use n=2 for computational purposes.

Equation (39) is then used in conjunction with the numerical solution of Eq. (11) (or the corresponding non-dimensional Eqs. (14) to (19)). By varying the input data and the type of particles, one can easily determine the behavior of the relative erosion rate against a certain parameter, such as the entrance flow velocity W, and the loading ratio Z. Since the most severe erosion prone area in pipe bends appears on the central plane of the pipe,[7] it is instructive and practical to confine our attention to the central plane as far as erosion is concerned. Also our analysis is restricted to the effect of the first impact of each particle stream at the wall. This region constitutes the primary wear point and is important in the design process.

RESULTS AND DISCUSSION

Mason[8] has measured the mean wear rate* for an an air-particle mixture flowing through a 90° elbow of 2" square section, having a d/D** ratio of 12. Hence, for comparison purpose, we choose a curved pipe of diameter 2" and a curvature ratio δ of 11. The physical properties of the mixture are also obtained from Mason.[8] Since we shall only present the results on the central plane of the curved pipe, the results are also applicable to a square sectioned pipe, provided the latter is assumed to be a two-dimensional system. This is because we have assumed that there is no secondary circulation of the flow field and a uniform entry condition. Particles will thus stay in the same plane throughout

---

* Defined as that quantity of powder which, when conveyed around a 90° bend, results in unit depth of wear at the primary wear point.

** See Fig. 6 for D and d.

the entire trajectory, as shown in Fig. 6. Thus by choosing a pipe diameter the same as the side of the square section, the solution for the particle equations of motion will be the same for both cases. Consequently, similar conclusions can be drawn from the central plane solution of the curved pipe and applied to the square section. It should be mentioned that the definition of erosion rate is different in the present case and in Mason.[8] Here we shall consider the maximum relative erosion rate, denoted by E_{max}, since this is the quantity which interests us most. However, we can still make a quantitative comparison with Mason.[8]

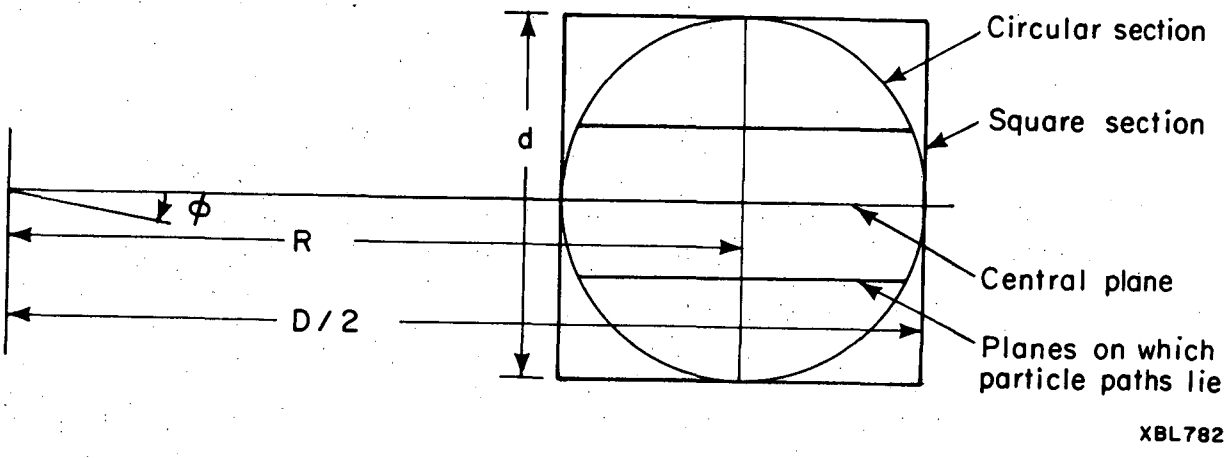

Figure 6. Similarity of the central plane of the circular section and the square section.

Figures 7 and 9 all give the erosion patterns of the central plane at a wide range of entry flow velocities. For velocities above 50 fps, the erosion patterns are similar and all confined to the range between $\phi = 0$ and $\phi = 36°$ approximately. A simple calculation based on the geometry of the particular curved pipe shows that $\phi = 33.6°$ is as far as particles can travel before their first impact with the wall, assuming the trajectories are straight lines. This suggests that under the prescribed conditions, particles with an initial velocity of above 50 fps will travel almost in a straight line and that there is negligible bending of paths due to the aerodynamic drag of the gas. If we calculate the parameter $\tilde{L}_m$ from (22), we find that for $W \geqslant 50$ fps, $\tilde{L}_m \geqslant 12$, which, as explained previously, indicates that particle paths will be relatively straight. The erosion pattern begins to stretch out to larger bend angle (Fig. 8) as W decreases. The stretching effect magnifies when the velocity drops to 5 fps, and, below 5 fps, some particles migrate out of the bend without any impact with the wall (Fig. 9). Figure 4 shows the variation of the maximum bend angle particles can travel with respect to entry velocity W. For practical purposes, we can calculate $\tilde{L}_m$ from the information in Fig. 10 and plot ϕ_{max} against $\tilde{L}_m$, as shown in Fig. 11. Since it has been shown that there are only two nondimensional parameters, $\tilde{L}_m$ and δ, in the governing equations, Fig. 11 is therefore applicable to all pipes with the same δ.

Figure 12 shows the variation of $\log_{10}(E_{max})$ versus $\log_{10}(W)$. It is found that at a velocity above approximately 8 fps, the slope of the plots are uniformly constant at a value of 3. Below 8 fps,

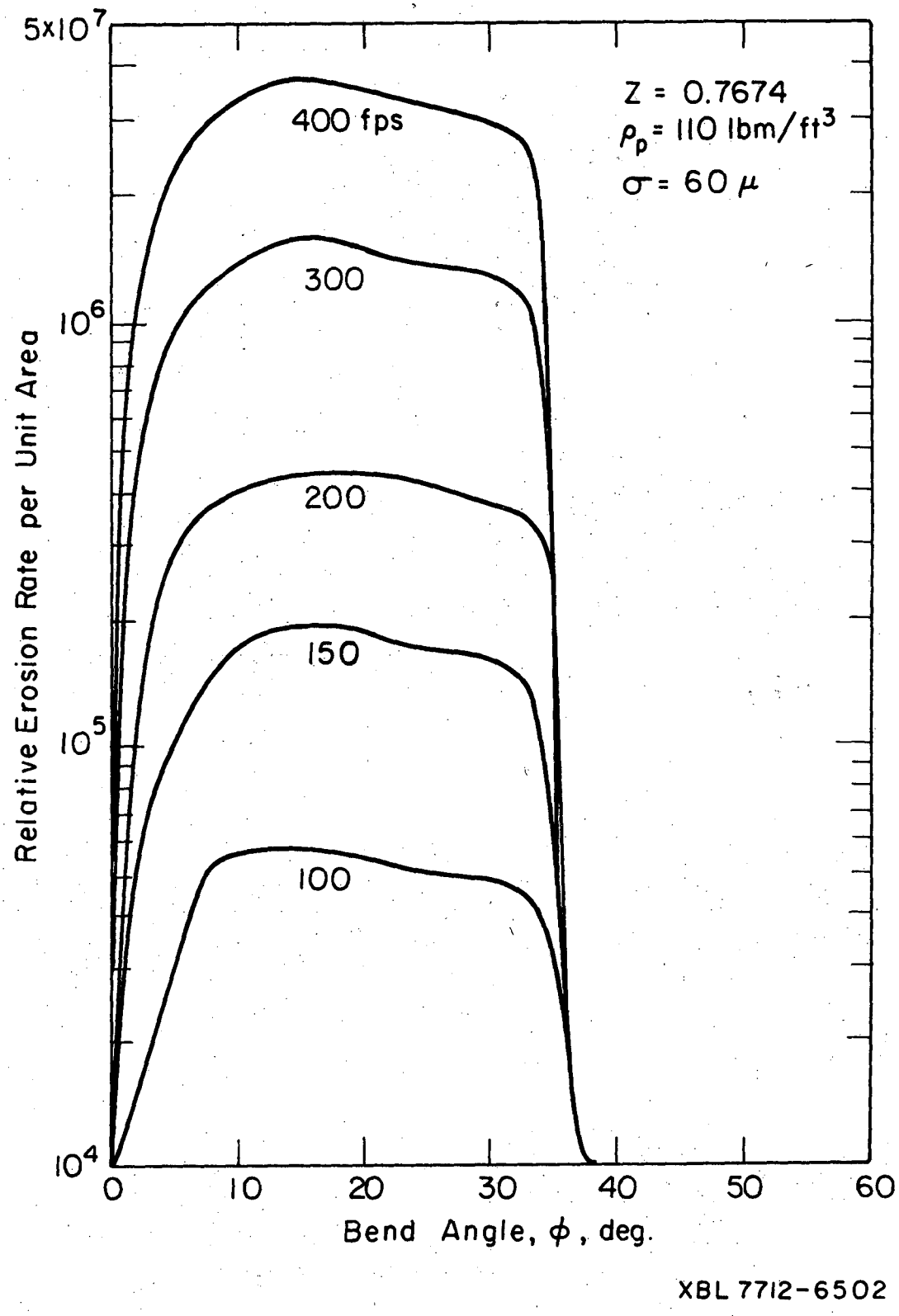

Figure 7 Variation of relative erosion rate per unit area along the central plane of the pipe wall.

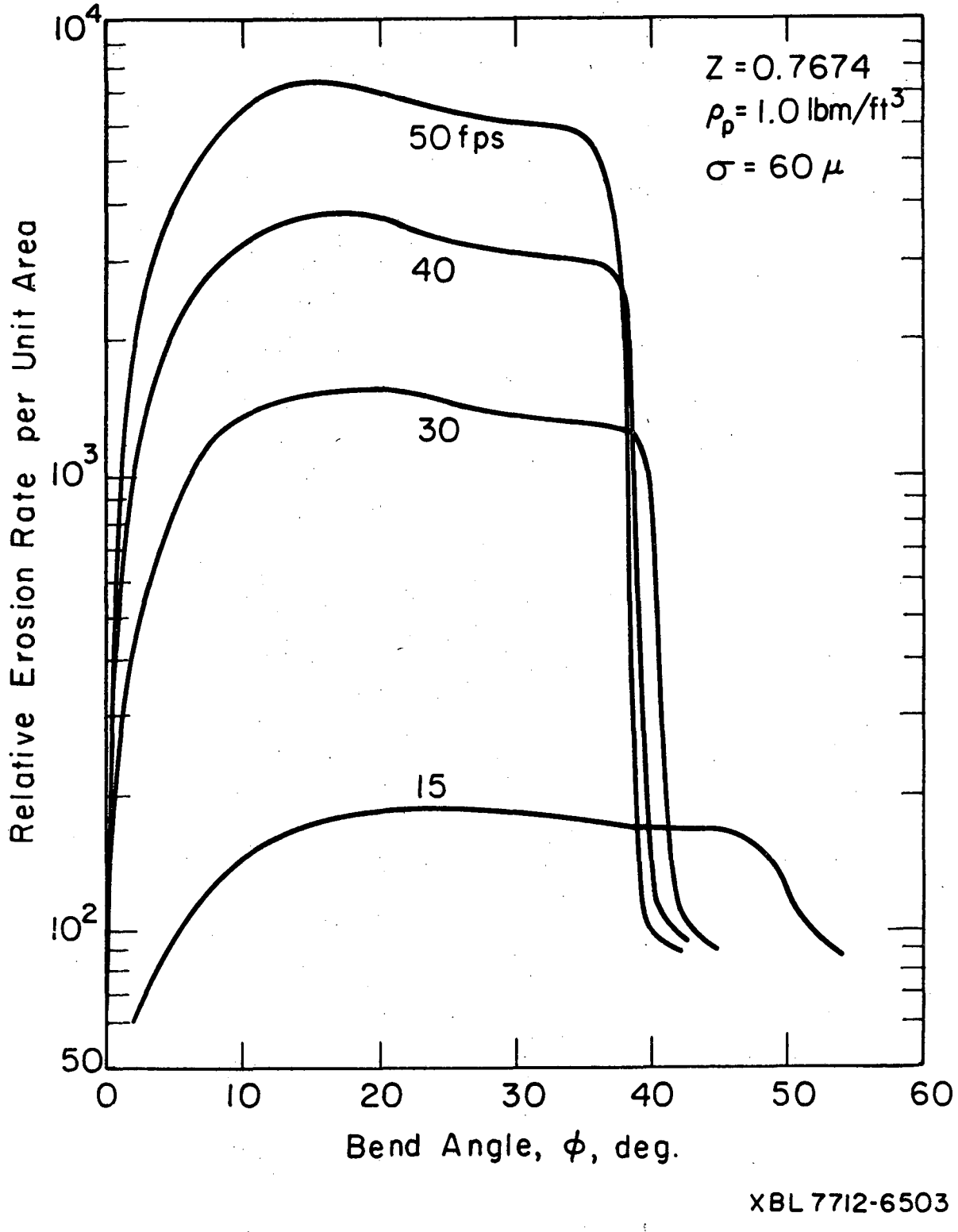

Figure 8 Variation of relative erosion rate per unit area along the central plane of the pipe wall.

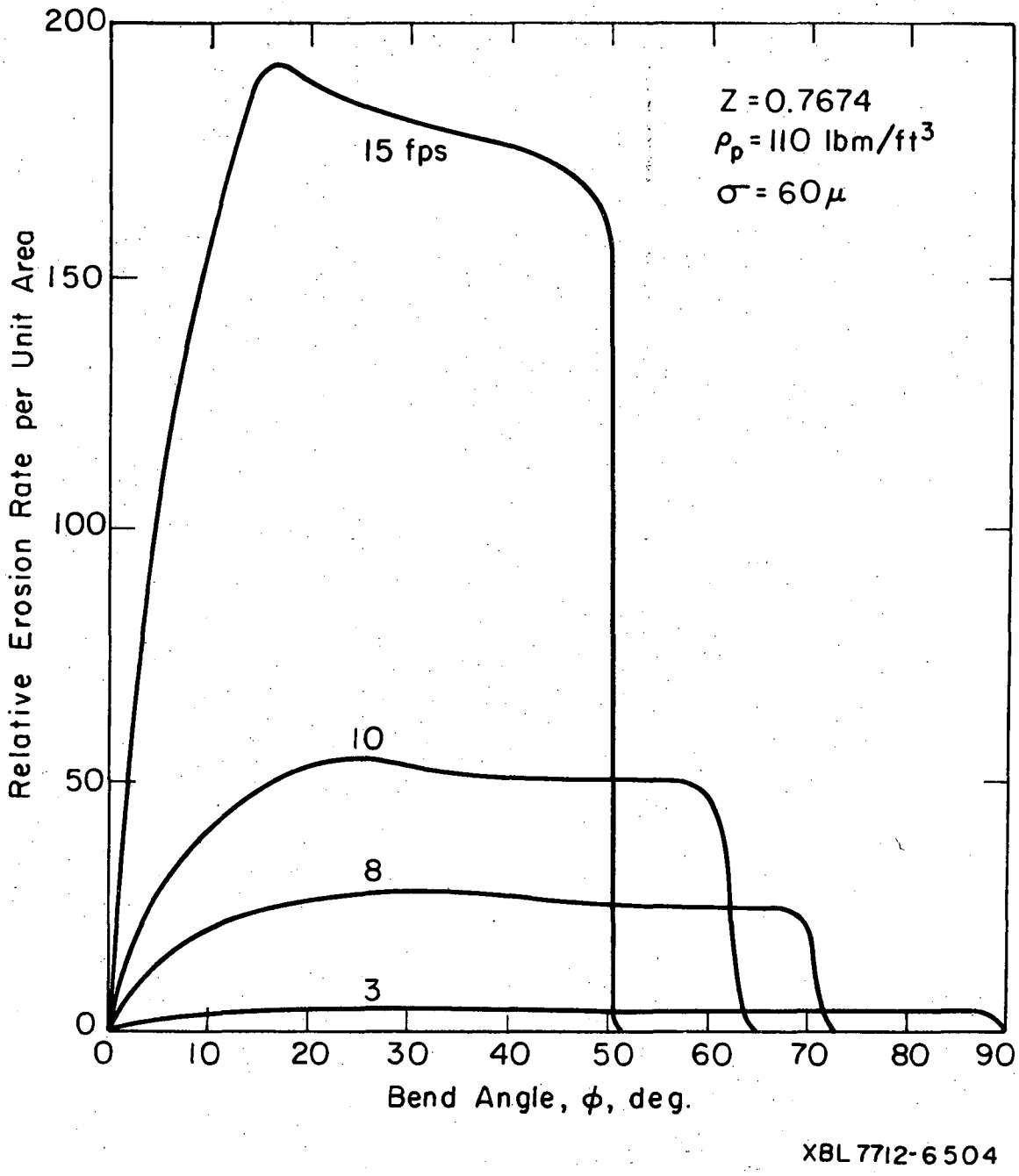

Figure 9 Variation of relative erosion rate per unit area along the central plane of the pipe wall.

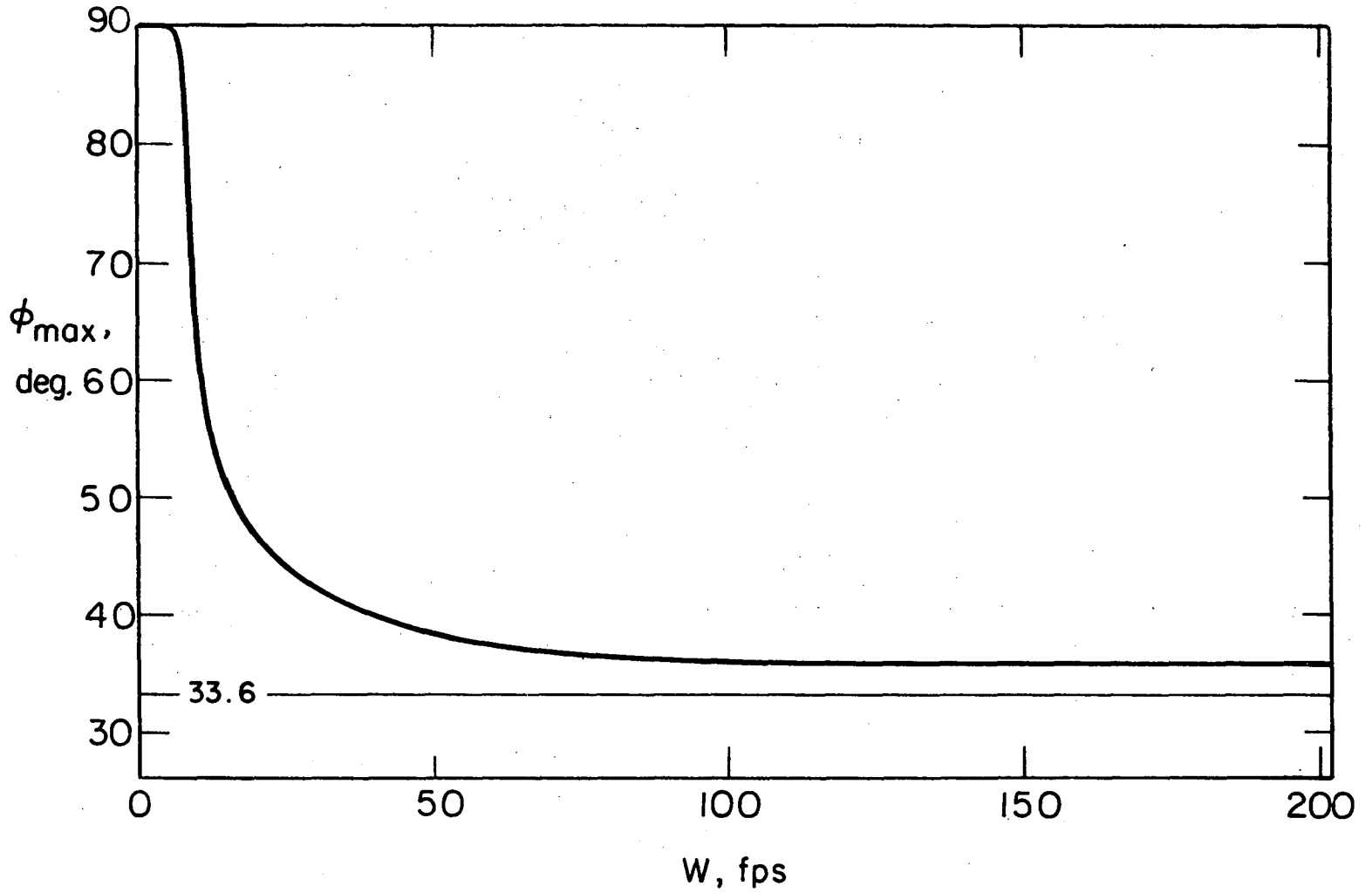

Figure 10 Dependence of region of erosion area on the central plane on entry velocity W for a curved pipe with a = 1" and δ = 11.

XBL 7712-6505

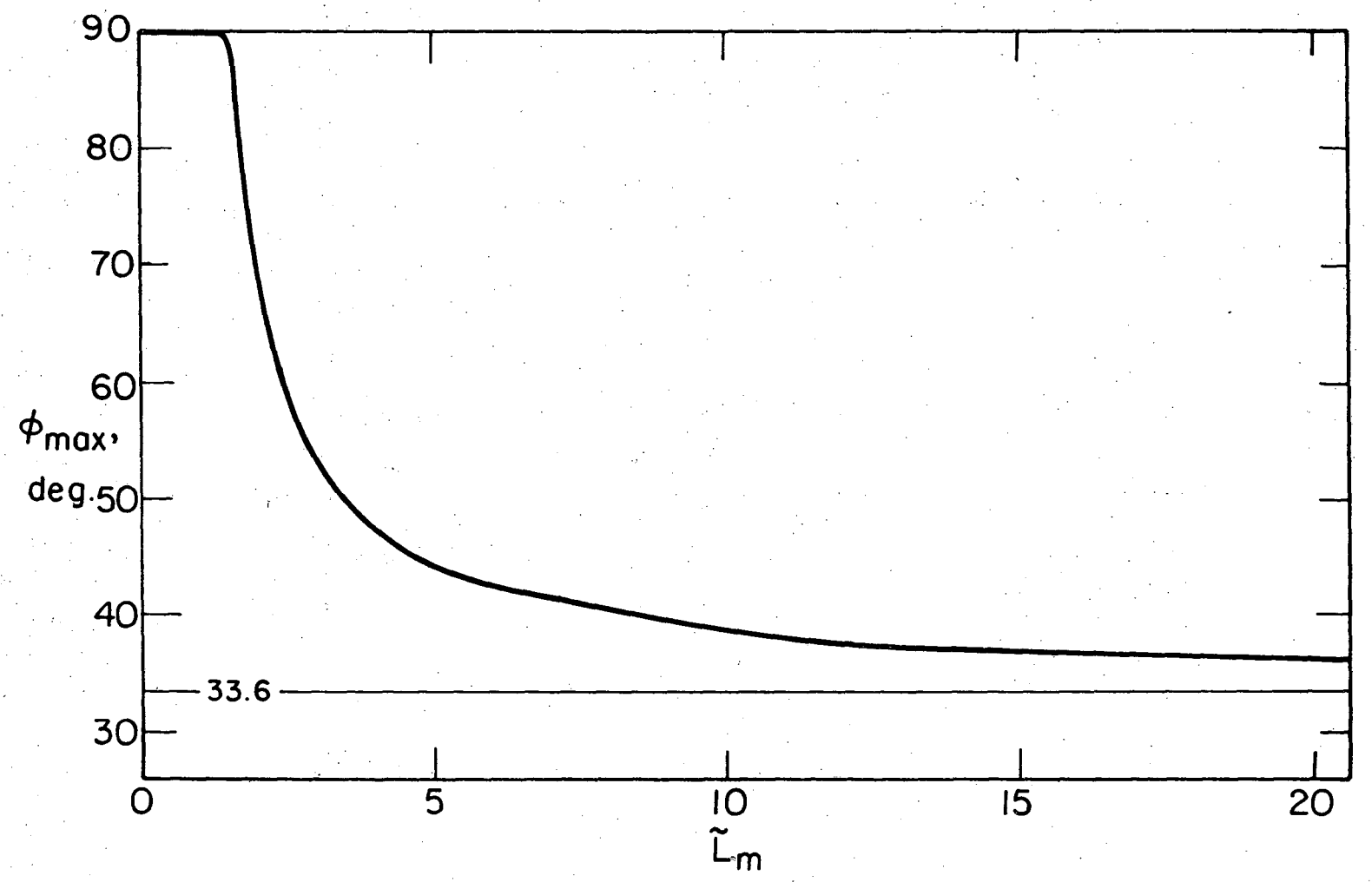

Figure 11 Variation of ϕ region of erosion area on the central plane against the non-dimensional momentum equilibration length $\tilde{L}_m$ for a curve pipe with $\delta = 11$.

XBL 7712-6506

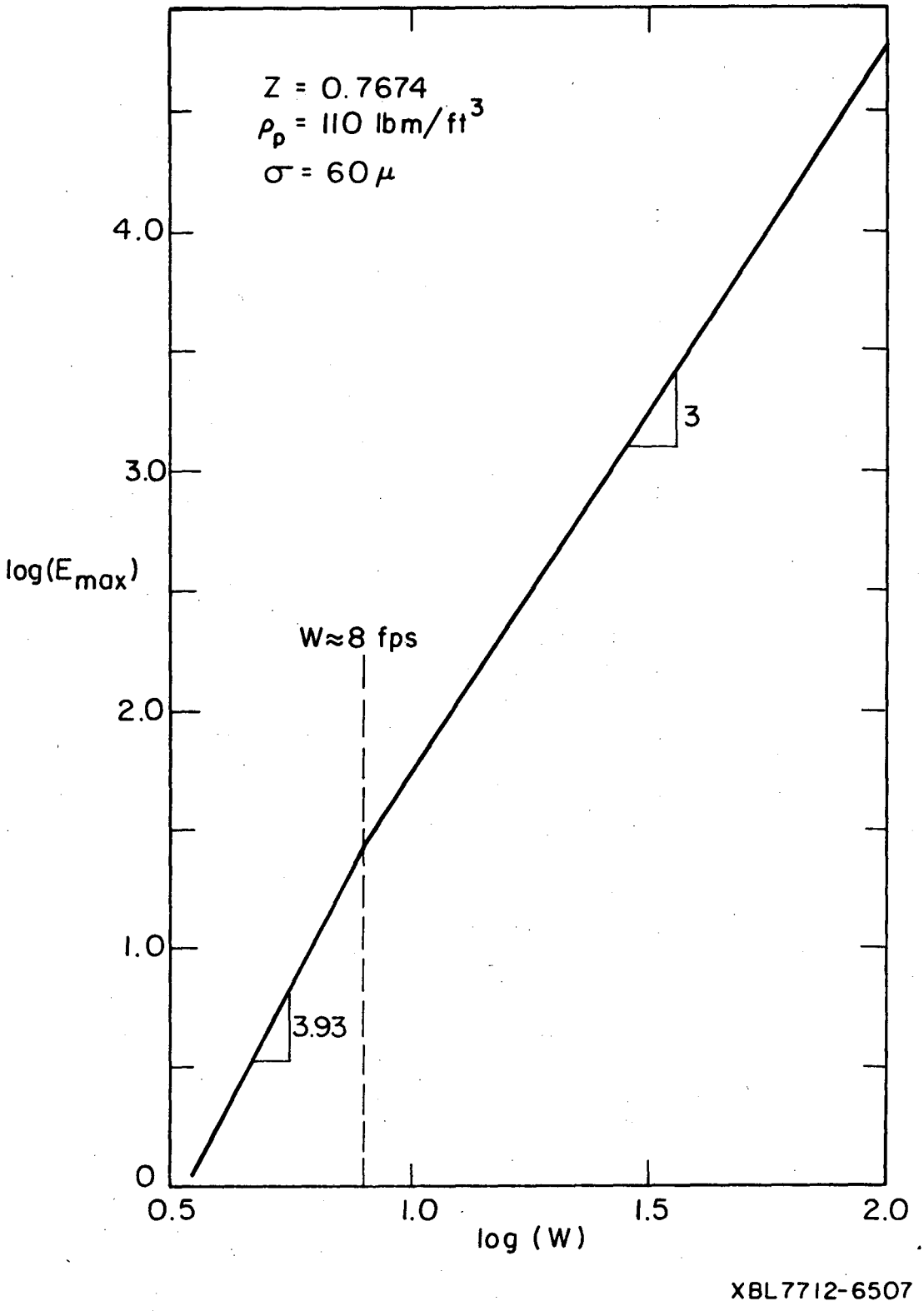

Figure 12 Dependence of maximum erosion rate on entry velocity.

the slope increases to about 3.93. This may be explained as follows. In Eq. (39), we can express P_k as

$$P_k = f\ W\ A_k(n,m)\ \tau_k \tag{40}$$

The residence time can be approximated by

$$\tau_k = D_k/Q_k \tag{41}$$

where D_k is the distance traveled by the kth trajectory across the cell. Substitute (40) and (41) into (39), we get

$$E = \frac{m_p}{VCELL} \sum_{k=1}^{i} f\ W\ A_k(n,m)\ \frac{D_k}{Q_k}\ Q_k^{n+1}\ F(\alpha_k) \tag{42}$$

For relatively large values of W, the effective momentum transfer of particle-fluid interaction is low[2] and thus the impact velocity Q is close to W. Hence

$$Q_k \cong W \tag{43}$$

Furthermore, since the paths are relatively straight, the impact angle α_k should not differ much, and, if we assume in addition that the sum $\sum_{k=1}^{i} A_k(n,m)\ D_k$ is roughly the same for those particle trajectories that cause the maximum erosion rate, we immediately arrive at the relationship

$$E_{max} \propto W^3 \tag{44}$$

for W large and n=2. For low velocities, the particle paths are bent more and more toward the gas streamlines, which are all parallel to the pipe surface. This causes the impingement angle to decrease sharply until it is less than 14°. Further lowering of velocities results in rapid decrease of the value $F(\alpha)$. Also the momentum transfer between phases is relatively effective for low velocity,[2] and the impact velocity will then be less than the initial velocity by a considerable amount. These two factors cause the E_{max} to drop more rapidly with W at the lower range of W than at the higher range. In this particular example,

$$\begin{aligned} E_{max} &\propto W^{3.93} \qquad \text{for } W \leq 8 \text{ fps} \\ E_{max} &\propto W^{3} \qquad \text{for } W > 8 \text{ fps} \end{aligned} \tag{45}$$

Next we shall consider the effect of varying the particle loading parameter, Z(% by weight of particles in mixture). In Fig. 13 $\log_{10}(E_{max})$ versus $\log_{10}(Z)$ is plotted for two velocities, 50 fps and 200 fps. It shows that for $Z \leq 0.5$, the curve (dotted lines) can very well be approximated by a straight line with a mean slope of about 1.34. At $Z > 0.5$, the curve takes off drastically, indicating the exponent on Z changes with Z itself. However, if we convert Z to Z_L mass ratio of particles to gas in mixture and replot $\log_{10}(E_{max})$ versus $\log_{10}(Z_L)$, the result is a straight line having a constant slope of 1 (Fig. 14). Thus we have further shown that

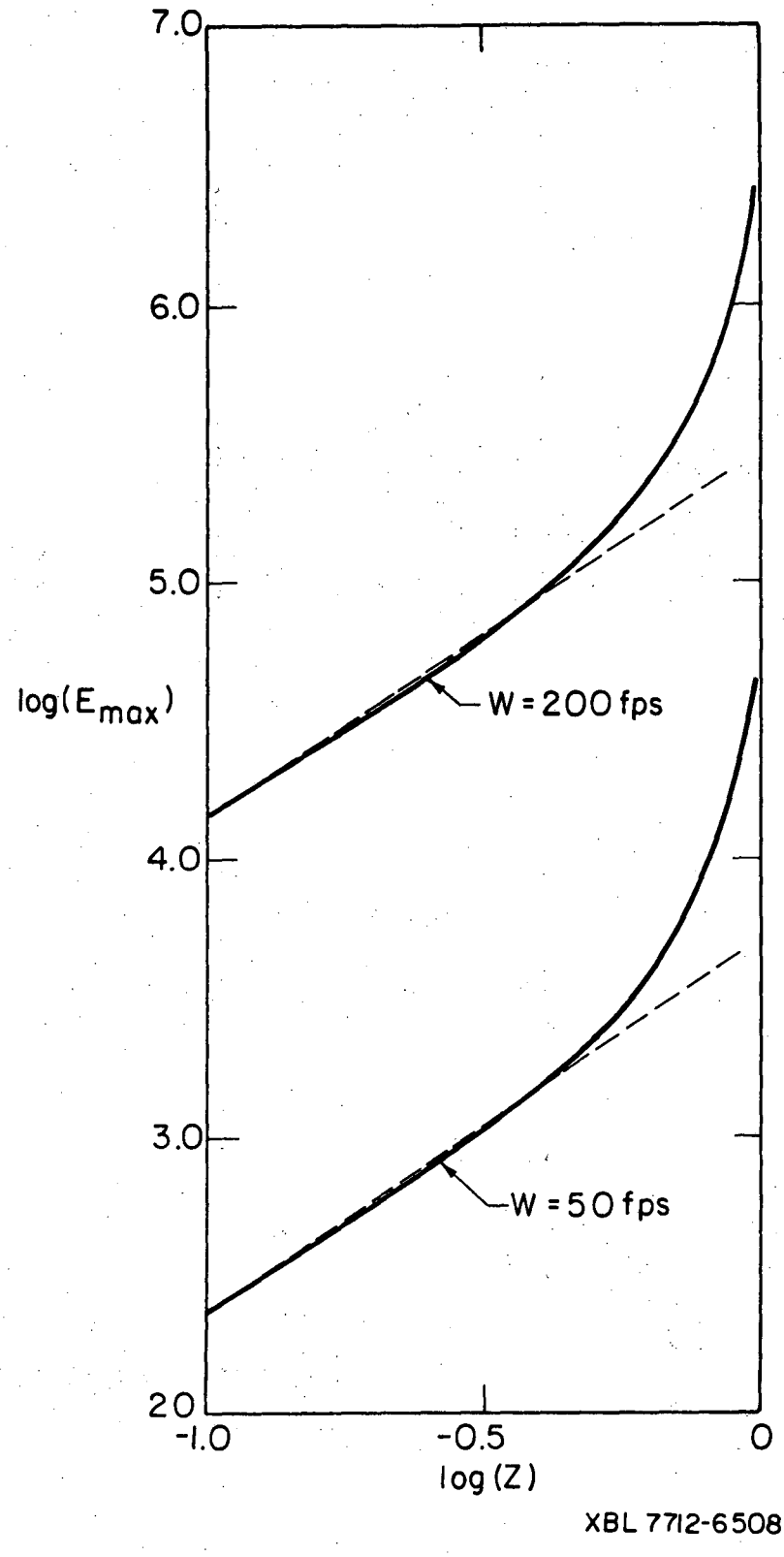

Figure 13 Dependence of maximum erosion rate on the loading ratio Z.

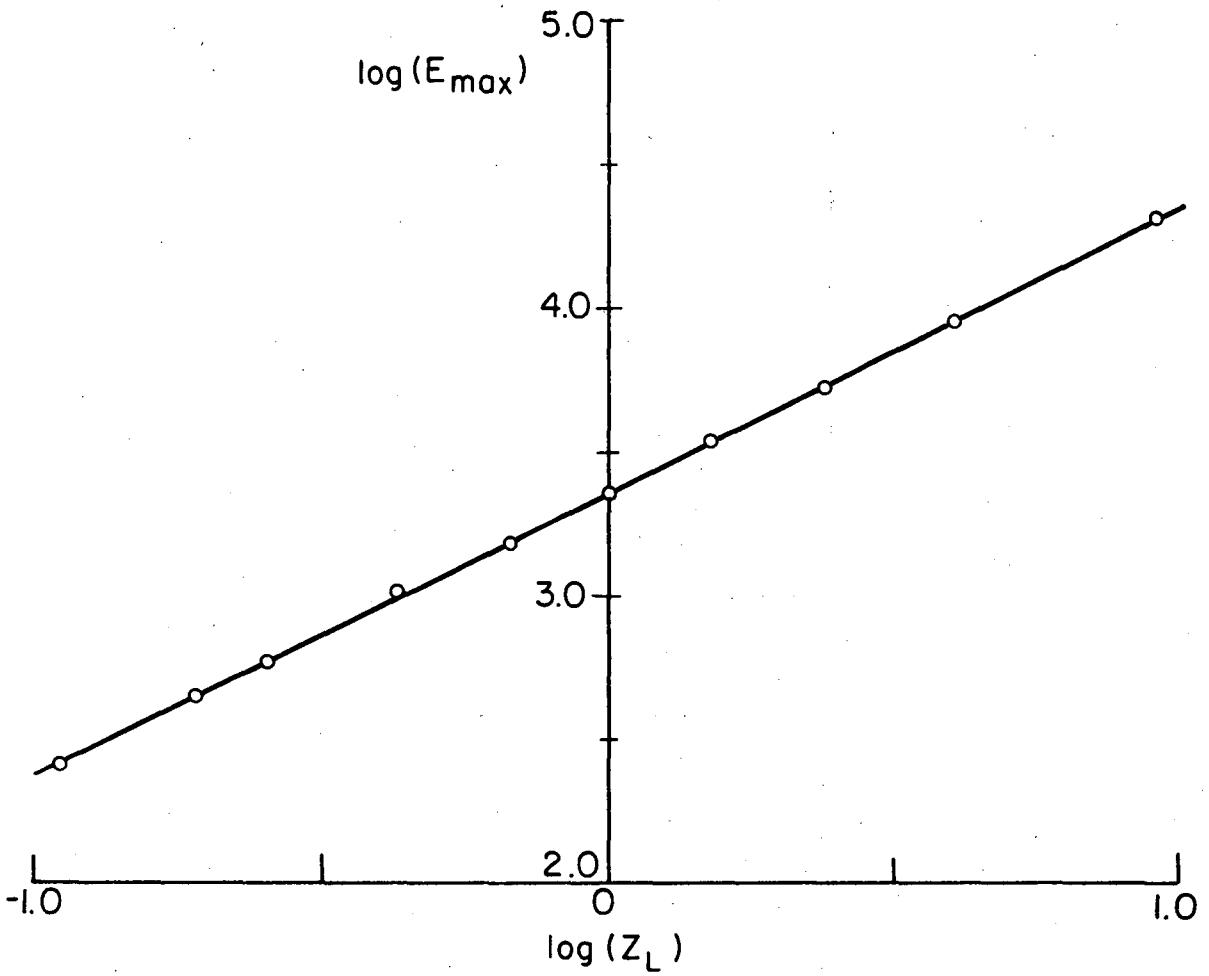

Figure 14 Dependence of maximum erosion rate on the loading ratio Z_L.

$$E_{max} \propto Z_L \tag{46}$$

and

$$E_{max} \propto Z^{1.34} \qquad \text{for } Z \leq 0.5 \tag{47}$$

At this point, the reader may wish to compare our results, given in Eqs. (45)-(47), with the equation given by Mason[8] for a dilute suspension namely

$$w \propto \frac{1}{W^{2.25} Z_L^{1.36}} \tag{48}$$

where w is the mean wear rate used by Mason, which was defined previously. From the definitions of E_{max} and W, we know that E_{max} is inversely proportional to W. Thus our results predict a higher exponent for W and a lower exponent for Z_L. However, they agree within a reasonable order of magnitude considering the simplicity of the analytical model.

CONCLUSION

The maximum relative erosion rate per unit area (E_{max}) at the central plane of a curved pipe of radius a = 2" and mean radius of pipe axis R = 11" is given by:

$$E_{max} \propto W^{3.93} Z_L \qquad \text{for } W \leq 8 \text{ fps}$$

$$E_{max} \propto W^{3} Z_L \qquad \text{for } W > 8 \text{ fps}$$

W is the flow velocity of the gas-particle mixture on entering the pipe and Z_L is the particle loading ratio (mass of particles/mass of gas). The analysis and theory are valid only for a dilute suspension.

The effect of other parameters, such as δ, ρ_p, or σ, can be similarly analysed numerically. We shall not pursue these further here since a quantitative trend can easily be deduced based on the theory already presented. Although the model is highly idealized, it gives reasonable results and provides a simple means of predicting the erosion pattern, the maximum erosion rate, and the region where erosion is most severe. It should be emphasized that the results are presented up to the first impact with the wall. Mason[8] indicated that secondary and tertiary wear points can easily occur especially in curved pipes with large curvature ratio and high flow rate. Any attempt to analyse beyond the primary wear point calls for very complicated methods. However, it is indicated that particles lose a considerable amount of kinetic energy upon impact[1] which may reduce their potential for erosion downstream. In addition, there is reason to believe that for loosely structured particles (such as coal char particles), the chance of attrition upon impact is great. This would further decrease the particles' abilities to erode. Consequently, the analysis up to the first wear point may in fact be adequate for applicational purposes.

FUTURE WORK

The present method employs a slug flow model for the gas phase and assumes that the presence of the particles does not affect the gas flow field. This is perhaps the simplest non-trivial case for gas-particle flow through a curved pipe. Furthermore, improvement of the solution calls for the removal of some of the ideal assumptions used in the present paper. There are three possible improvements which are discussed in the following:

(1) Assuming the flow is fully developed in the curved pipe and accounting for all other effects, such as the momentum coupling between the particle and the gas phase, viscosity effect of the gas, gravity effect, etc., enables one to eliminate one independent variable and the resulting formulation becomes two-dimensional. However, it is questionable that a gas-particle mixture flowing in a curved pipe can ever attain a fully developed state. Furthermore, the entry length in a curved pipe is not small[4] so that for a typical 90° pipe bend, the entry region may in fact be the more important region of interest, especially when one is interested in erosion estimation.

(2) We still assume that the presence of particles does not affect the gas flow field, but instead of using a slug flow model for the gas flow field, we make use of the existing solution for the entry flow of a viscous fluid into a curved pipe, such as that by Yao.[4] However, since all such existing solutions are obtained numerically, it presents a difficulty in the computer solution of the particle phase equations of motion. Also those solutions are very approximate and the uncertainty induced may be just comparable to using a slug flow model.

(3) Formulate the problem in three dimensions, taking into account the momentum coupling, viscosity effect and other effects which may play an important role in the formulation.

Improvement (3) is thus the logical approach one should follow beyond the present method. The feasibility of obtaining solutions from the complete formulation should be the main consideration in following this approach, apart from the fact that the correct formulation of a gas-particle flow is quite difficult. Other questions which have to be clarified before attempting such an approach are the nature of flow (Laminar or Turbulent), the continuum approximation, and the boundary conditions.

ACKNOWLEDGMENTS

Special thanks are due to Prof. I. Finnie for useful discussions. This work was supported by the Division of Basic Energy Science of the Department of Energy, with A. Levy as Program Manager and M. Holt as Faculty Advisor.

REFERENCES

1. I. Finnie, Wear 19, 81 (1972).

2. S.L. Soo, Fluid Dynamic of Multiphase Systems (Blasidell Pub. Co., Waltham, Mass., 1967).

3. S.L. Soo, Physics of Fluid 18, 263 (1975).

4. L.S. Yao, "Entry Flow in a Curved Pipe," Ph.D thesis, Univ. of California (1973).

5. S.L. Soo, Phy. Fluid 20, No. 4, 568 (1976).

6. C.T. Crowe and D.T. Pratt, Proc. 1972 Heat Tran. Fluid Mech. Inst., (Stanford University Press, 1972), 23.

7. I. Finnie, private communication.

8. S. Mason and B. V. Smith, Powder Tech. 6 (1972), 323.

TECHNICAL INFORMATION DEPARTMENT
LAWRENCE BERKELEY LABORATORY
UNIVERSITY OF CALIFORNIA
BERKELEY, CALIFORNIA 94720